

“Navigate-dock-activate” anti-tumor strategy: Tumor micromilieu charge-switchable, hierarchically activated nanoplatform with ultrarapid tumor-tropic accumulation for trackable photothermal/chemotherapy

Kondareddy Cherukula¹, Saji Uthaman², In-Kyu Park^{1*}

1. Department of Biomedical Science and BK21 PLUS Centre for Creative Biomedical Scientists, Chonnam National University Medical School, Gwangju 61469, Republic of Korea.
2. Department of Polymer Science and Engineering, Chungnam National University, 99 Daehak-ro, Yuseong-gu, Daejeon 34134, Republic of Korea

*To whom correspondence should be addressed : In-Kyu Park , e-mail: pik96@jnu.ac.kr

Supporting Information

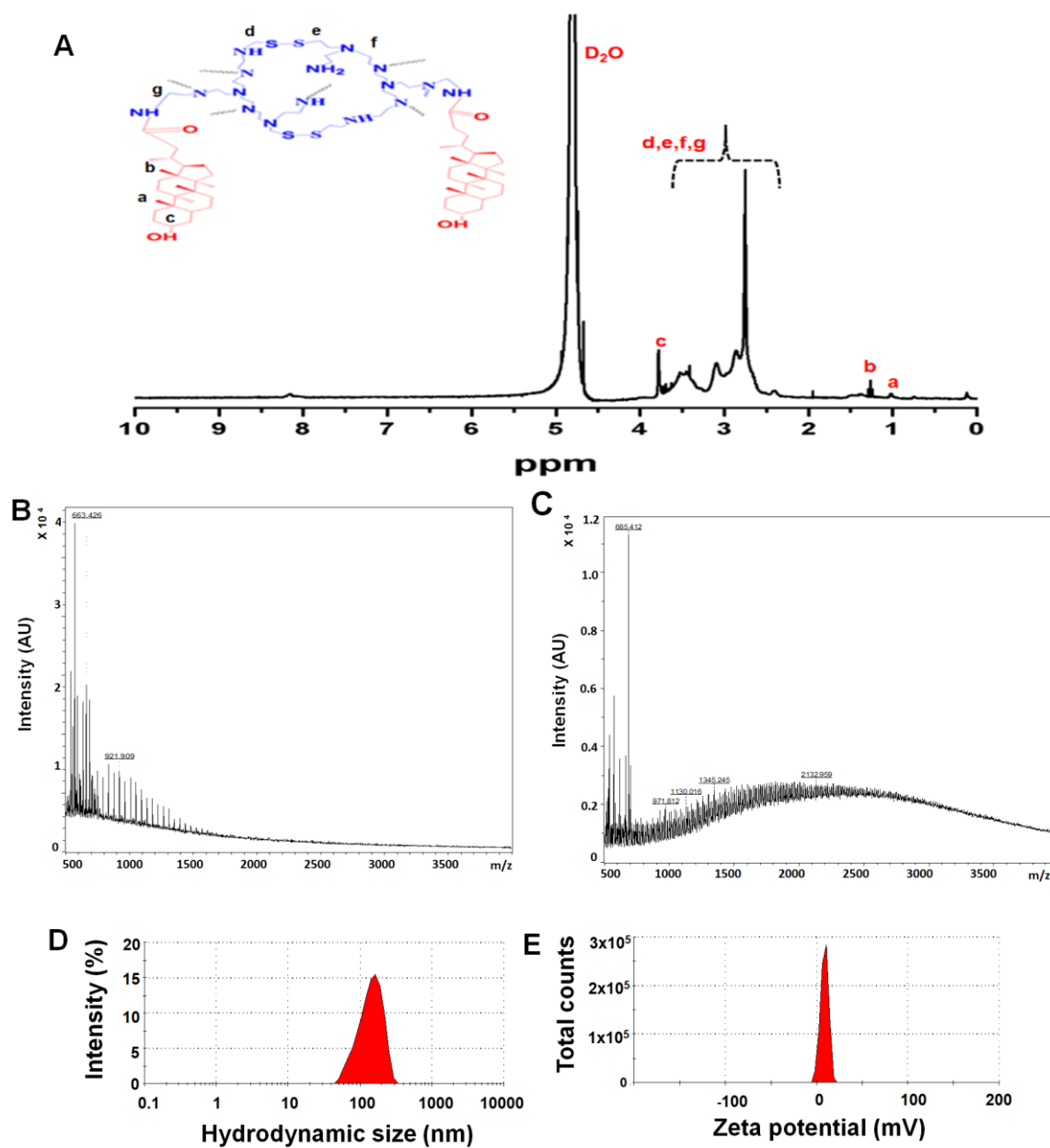


Figure S1. (A) ¹H NMR analysis of LAPMi. MALD-TOF analysis of ssPEI (B) and LAPMi treated TCEP (C). DLS analysis of LIL-PTX NPs demonstrating the (D) hydrodynamic size and (E) zeta potential.

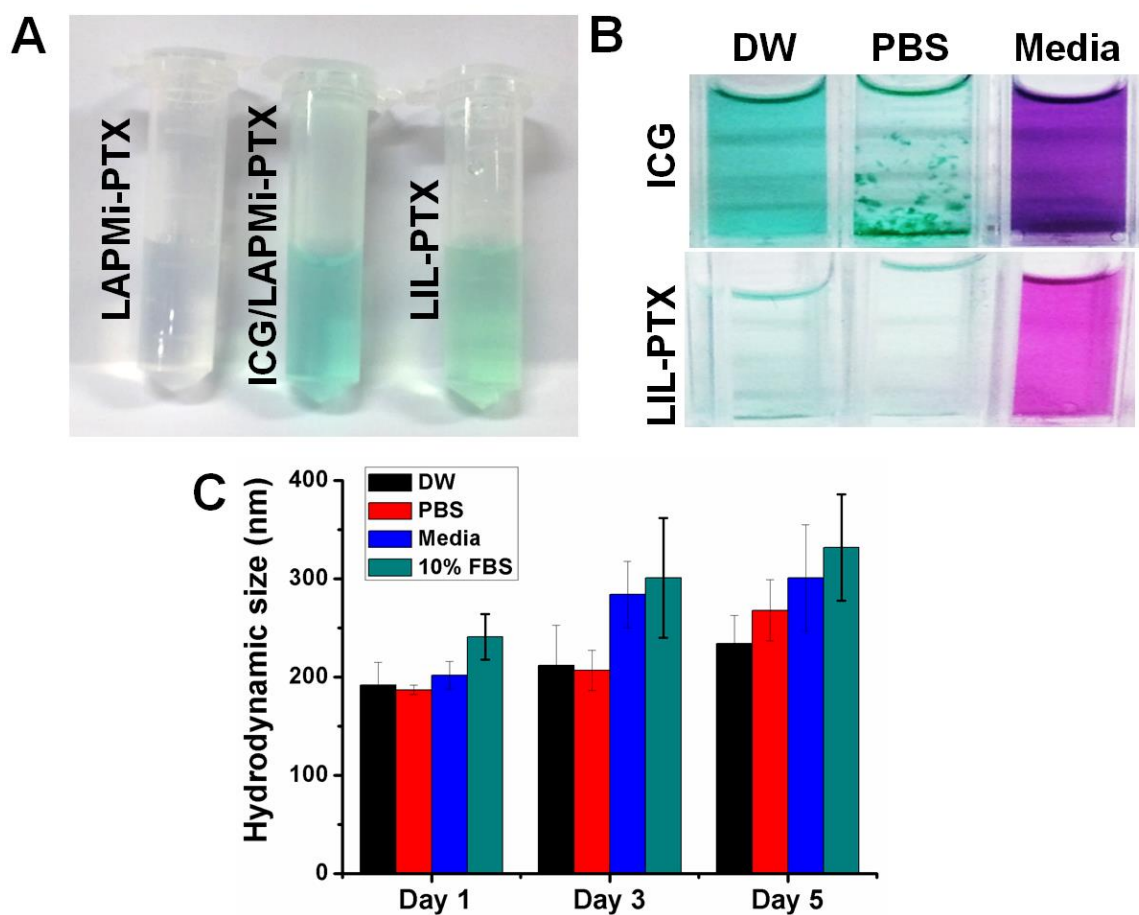


Figure S2. Digital images of as-prepared nano formulations in (A) DW and (B) different media. (C) Hydrodynamic size changes of LIL-PTX for 5 days in different buffer and serum conditions.

Fig. S2 showed that good dispersion ability of all the formulations in the aqueous solution. Also, addition of ICG in PBS showed precipitation, indicating their physiological instability. On the other hand, LIL-PTX showed enhanced stability in PBS, DW and culture media conditions.

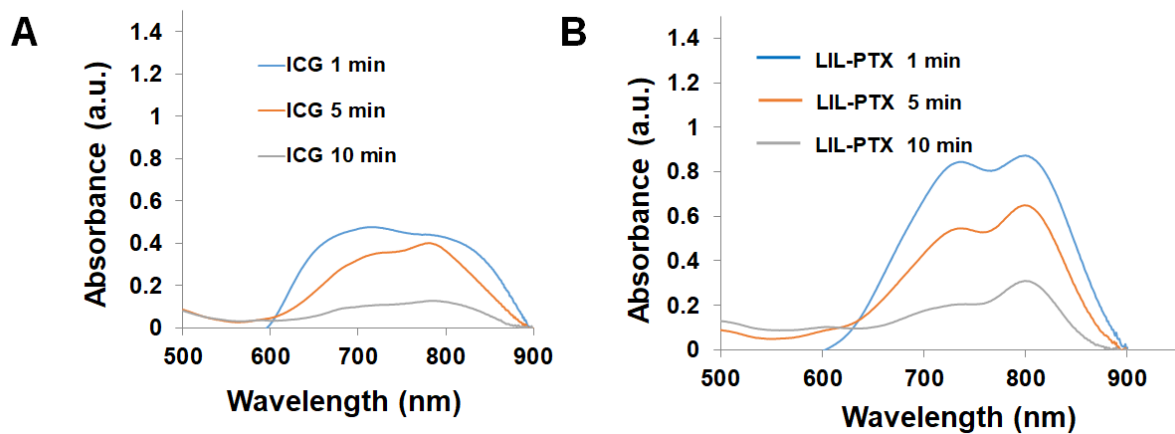


Figure S3. UV-VIS absorbance graph of ICG (A) and LIL-PTX NPs (B) upon laser irradiation (808nm, 2W/cm²) at different time point of irradiation.

Fig.S3 suggested that bare ICG witnessed a lower NIR absorbance compared with LIL-PTX NPs upon laser irradiation. This indicated that the LIL-PTX NPs as a stable and efficient nanoagent for PTT.

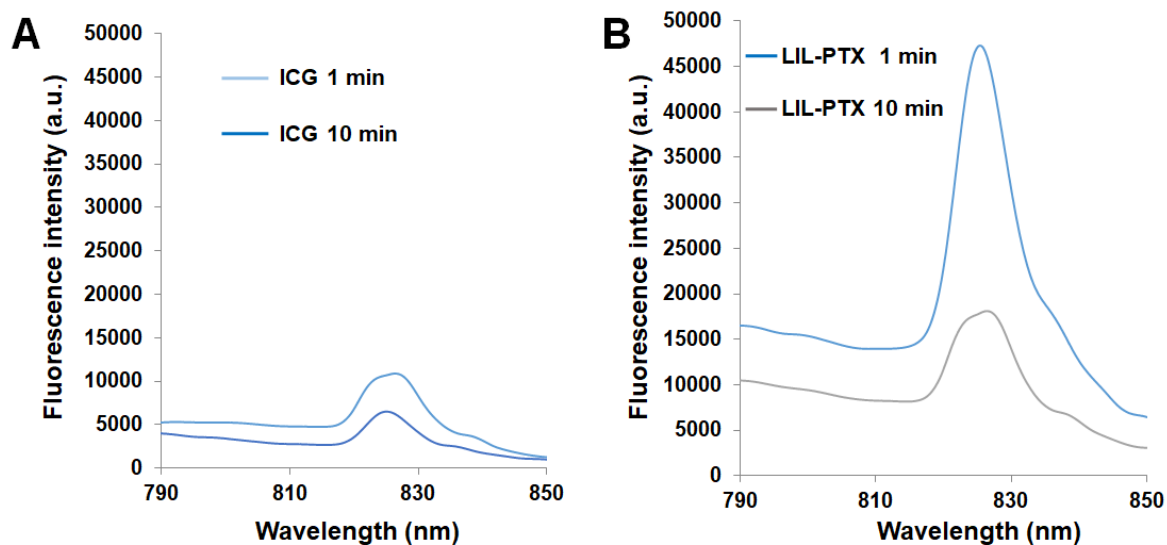


Figure S4. Fluorescence spectrum of ICG (A) and LIL-PTX NPs (B) upon laser irradiation (808nm, 2W/cm²) at different time point of irradiation.

Fig.S4 showed that ICG undergone photodegradation upon laser irradiation, whereas, LIL-PTX realized lower photodegradation compared with bare ICG. This demonstrated that ICG encapsulated LIL NPs is highly stable and undergoes lower photodegradation, indicating LIL-PTX as an efficient PTT agent.

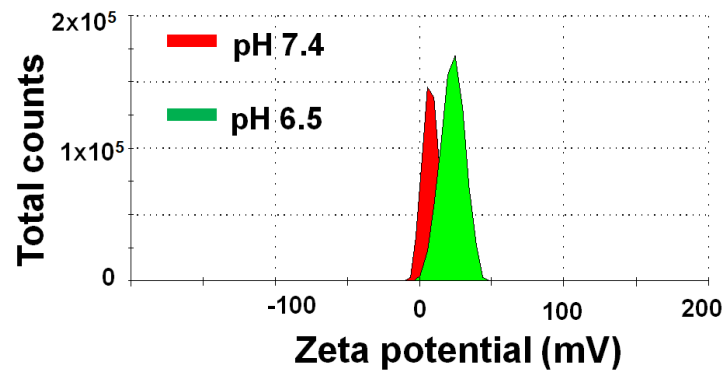


Figure S5. Zeta potential graph of LIL-PTX NPs at acidic pH of 6.5 and physiological pH 7.4.

Fig.S5 showed a surface charge switch of LIL-PTX NPs, at slightly acidic tumor milieu (pH 6.5), presumably due to the protonation of amines.

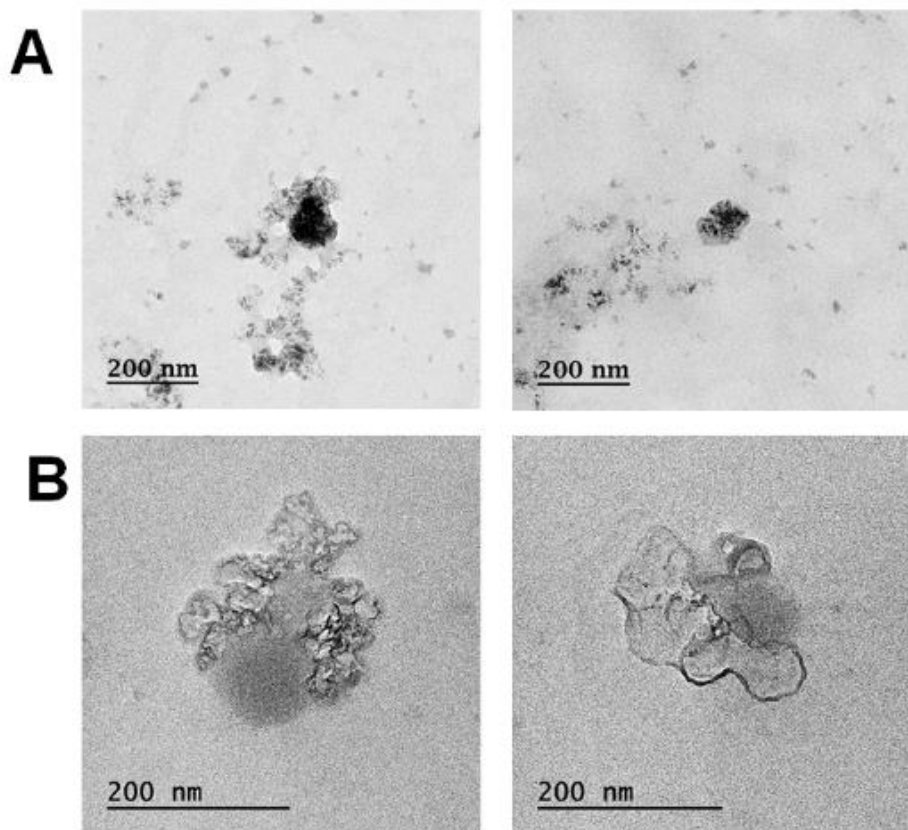


Figure S6. FE-TEM image of (A) LIL-PTX NPs irradiated with laser (808nm, 2W/cm², 10 min) incubated in DMEM (pH 6.5) and (D) FE-TEM image of irradiated samples with GSH (10mM) incubation in DMEM (pH 6.5).

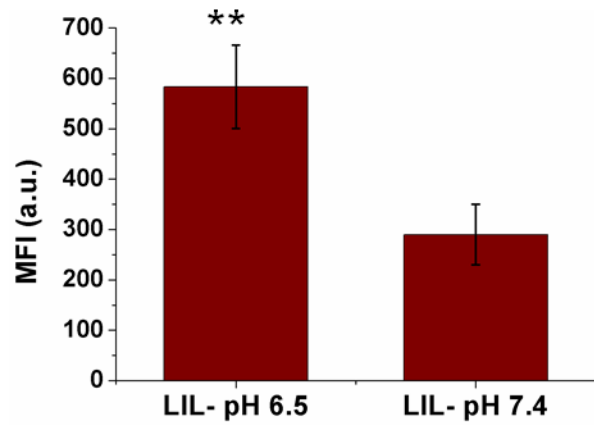


Figure S7. Mean fluorescence intensity quantification of CT26 cells treated with LIL NPs at pH 7.4 and 6.5 measured by flow cytometry analysis (** $p < 0.01$).

Fig. S7 showed that LIL NPs demonstrated an enhanced intracellular uptake in the acidic pH 6.5, compared with pH 7.4, due to the enhanced interaction of positively charged LIL NPs with the cancer cells at acidic pH 6.5.

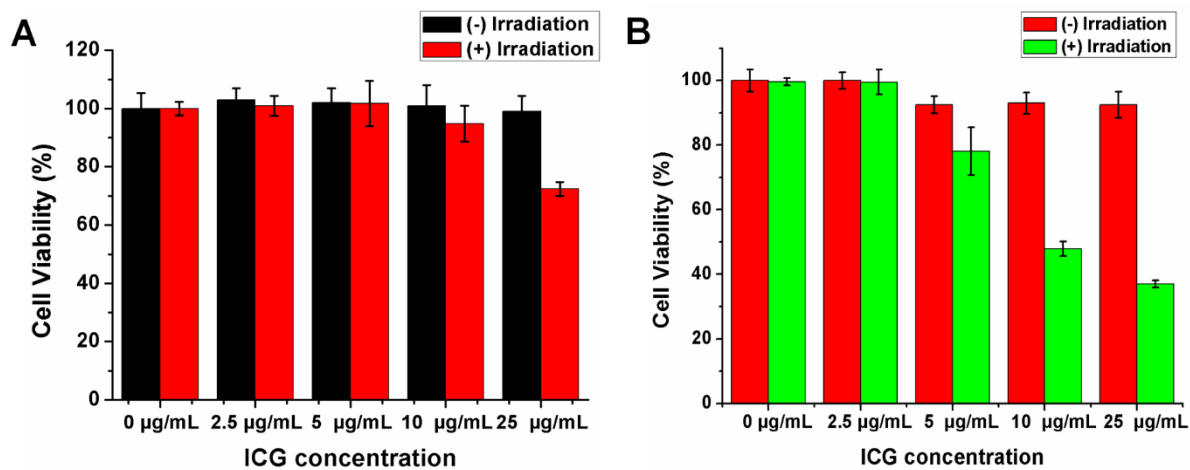


Figure S8. (A) Cell viability of CT26 cells incubated with ICG for 24h with and without laser irradiation (808nm, 2W/cm², 10 min). (B) Cell viability of CT26 cells incubated with LIL NPs for 24h with and without laser irradiation (808nm, 2W/cm², 10 min).

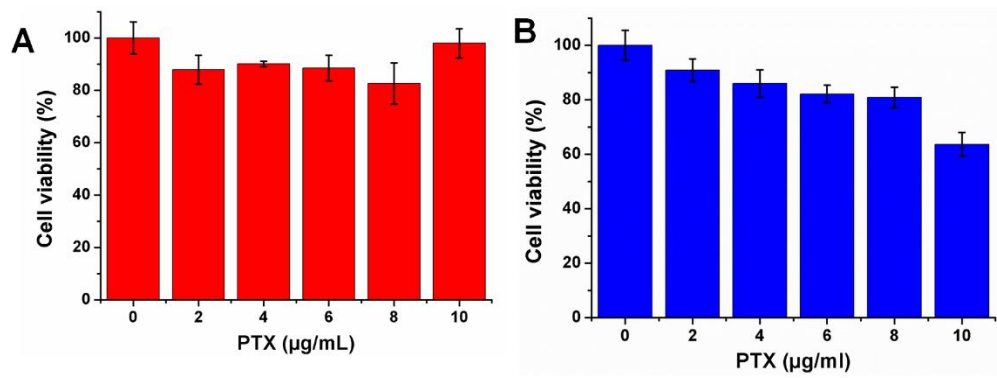


Figure S9. (A) Cell viability of CT26 cells incubated with PTX for 24h. (B) Cell viability of CT26 cells incubated with LIL-PTX NPs.

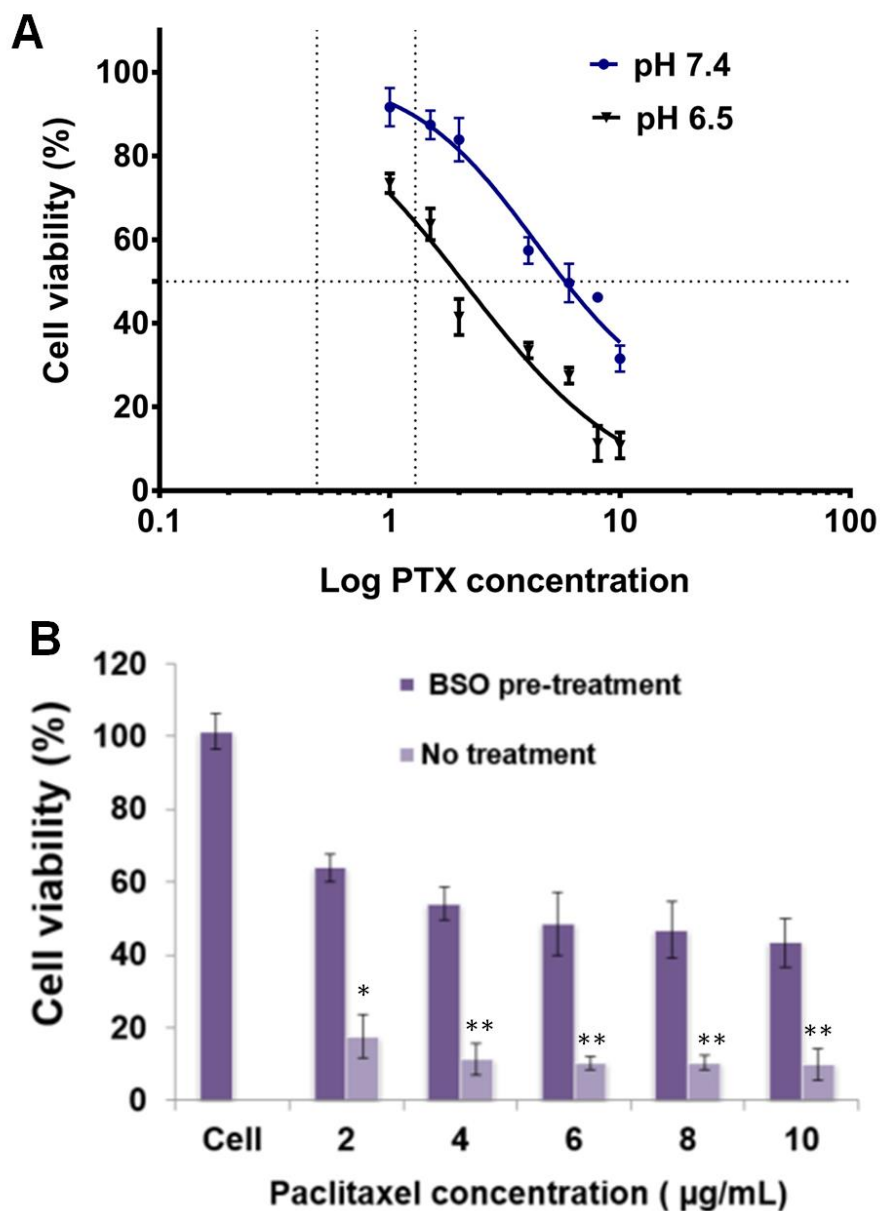


Figure S10. (A) Dose responsive curves of LIL-PTX NPs treatment for 24h with and without laser irradiation (808nm, 2W/cm², 10 min) at pH 7.4 and pH 6.5. (B) Cell viability of CT26 cells incubated with LIL-PTX NPs for 24h with and without BSO pre-incubation subjected to laser irradiation (808nm, 2W/cm², 10 min) (* $p < 0.05$ and ** $p < 0.01$).

Fig.S10B showed that BSO-mediated intracellular glutathione inhibition evidenced low cellular toxicity compared with the non-BSO pre-treated control, indicating GSH as an efficient endogenous trigger for drug release.

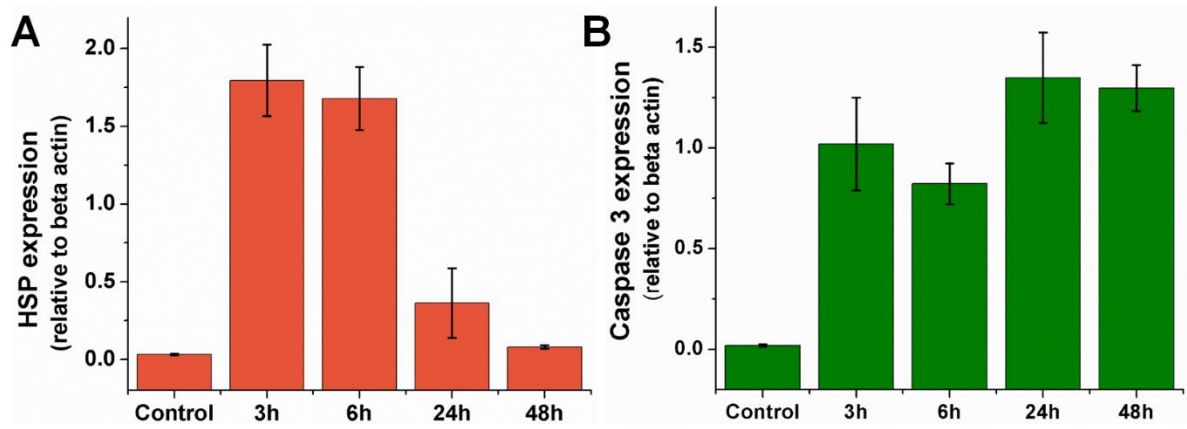


Figure S11. (A) Relative HSP 70 levels and (B) relative caspase 3 levels measured from western blot of CT26 cells incubated with LIL-PTX NPs for 24h with and without laser irradiation (808nm, 2W/cm², 10 min).

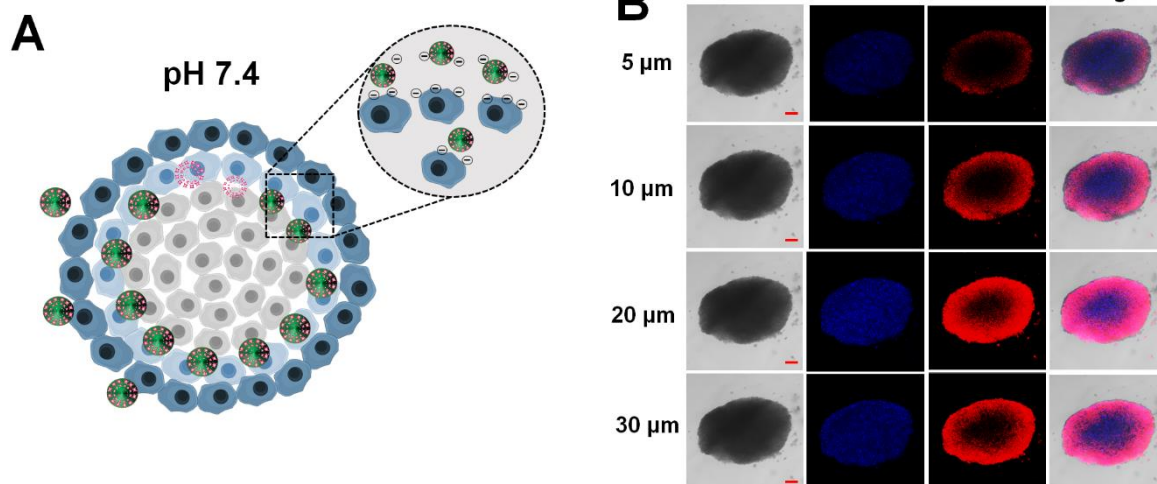


Figure S12. Multicellular tumor spheroid of CT26 cells incubated with the ICG/LAPMi-PTX for 4h at pH 6.5.

Fig.S12 demonstrated a lower penetration in the tumor spheroid and mainly accumulated in the periphery of spheroid.

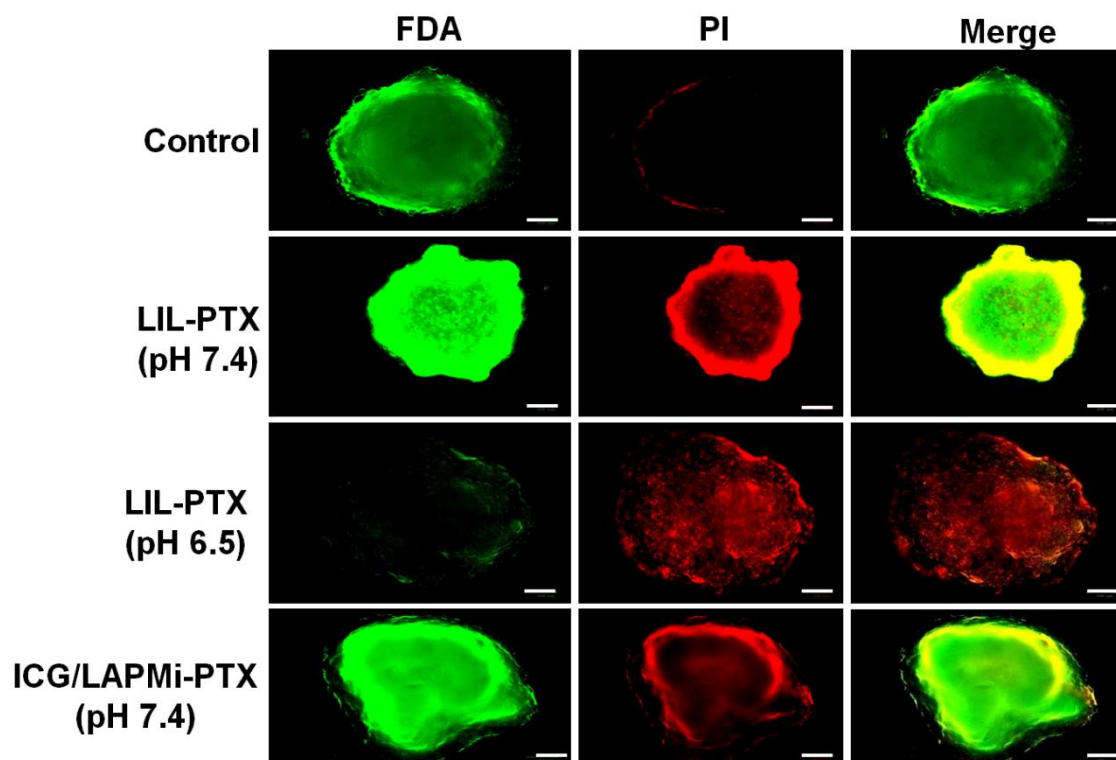


Figure S13. Live/dead assay in multicellular tumor spheroid of CT26 cells incubated with the LIL-PTX NPs and ICG/LAPMi-PTX for 4h. Scale bar is 100 μ m.

Fig.S13 demonstrated that presence of lipid and acidic pH 6.5, as an important parameters in the tumor penetration and eliciting enhanced cancer cell death.

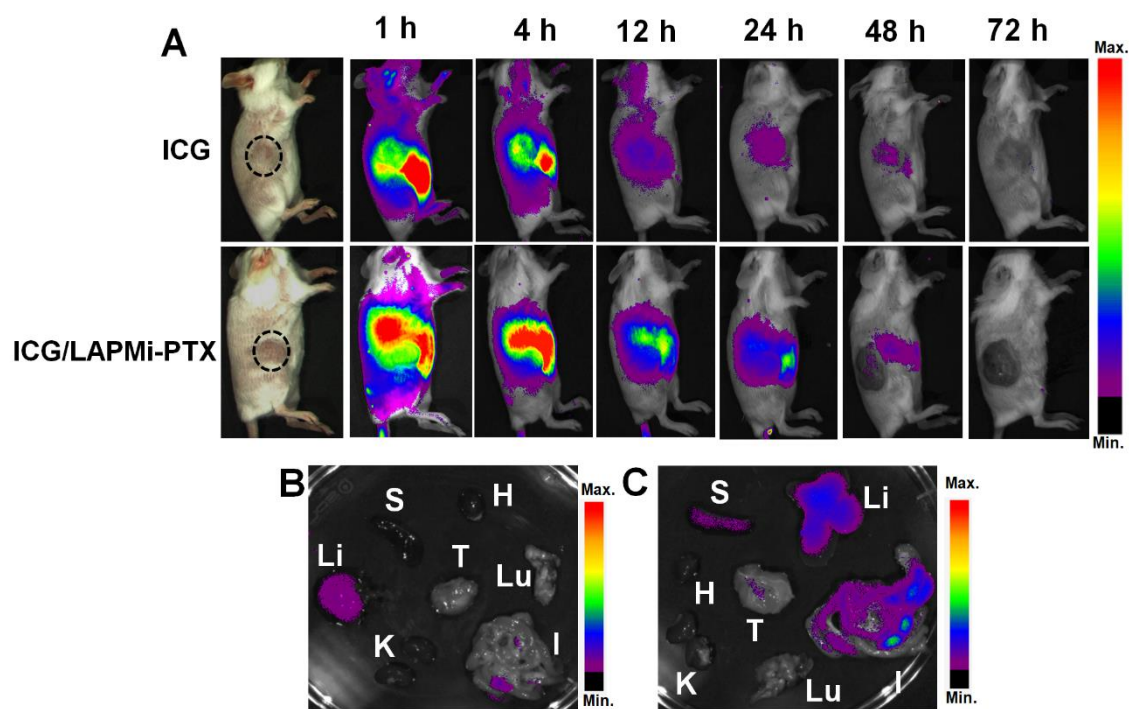


Figure S14. (A) Biodistribution of ICG (1.5mg/kg) and ICG/LAPMi-PTX (1.5mg/kg of ICG) injected via tail vein in CT26 tumor bearing mouse. (B) *Ex vivo* images of mice collected from LIL NPs injected mouse after 24h post-injection injection (K: kidney, Lu: lung, Li: liver, S: spleen, I: intestine, T: tumor, H:heart).

Fig.S14 showed that the bare ICG and ICG/LAPMi-PTX was not able to home to tumor region, reaffirming the role of PEG lipids in enhanced circulation and tumor accumulation.

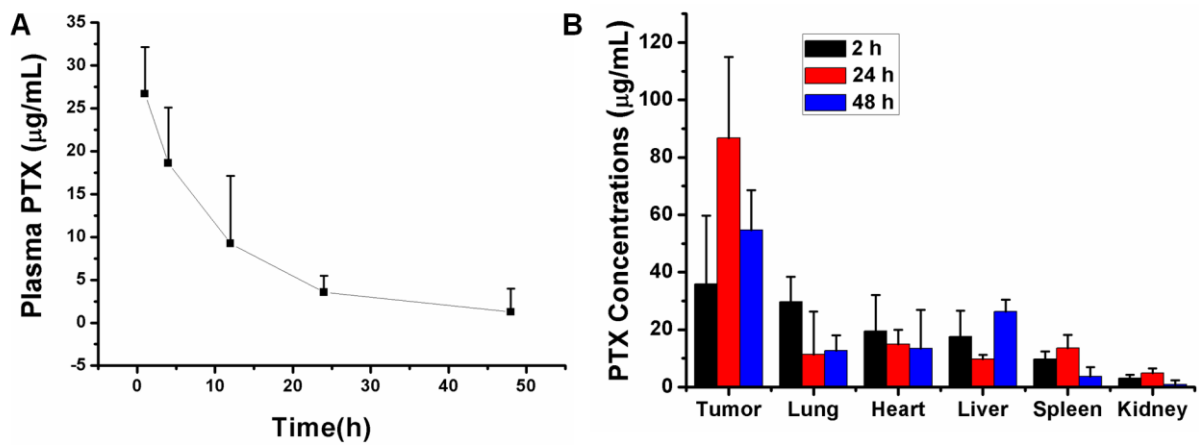


Figure S15. (A) Plasma PTX concentration-time curves after intravenous administration of LIL-PTX (10 mg/kg of PTX). (B) Biodistribution of PTX in tumor, lung, heart, liver, spleen and kidney after intravenous injection of LIL-PTX (10mg/kg of PTX).

Table S1. Pharmacokinetic parameters of LIL-PTX administration through intravenous route

Parameters	LIL-PTX
$t_{1/2}$ (h)	10.76
AUC ($\mu\text{g}\cdot\text{h}/\text{mL}$)	39.66
CL (L/h)	0.117

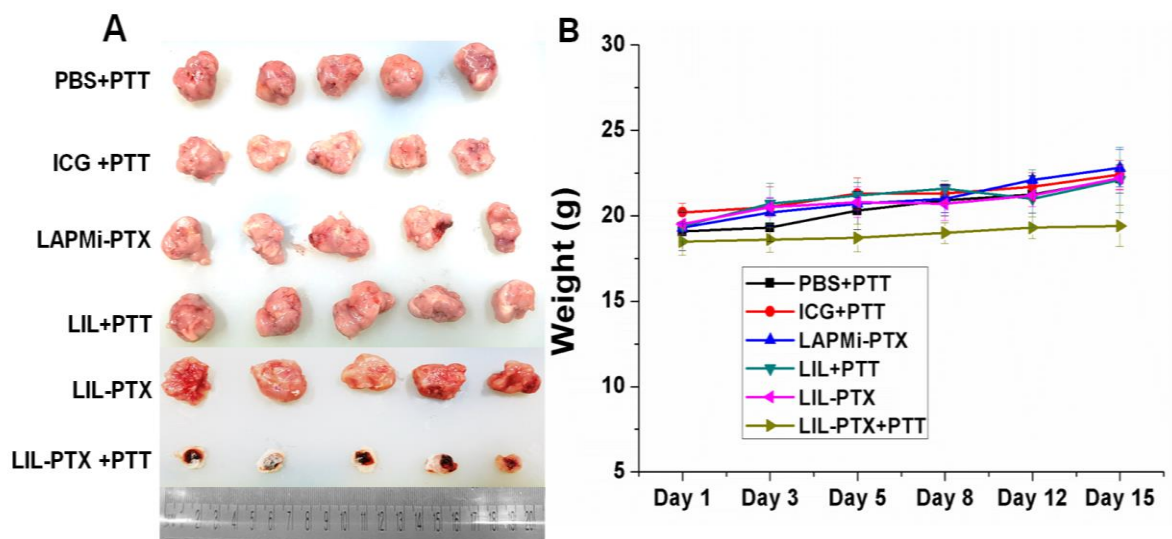


Figure S16. (A) Representative images of tumor dissected from various groups 14 day post-treatment. (B) Mice body weight changes for treatment period of 14 days.

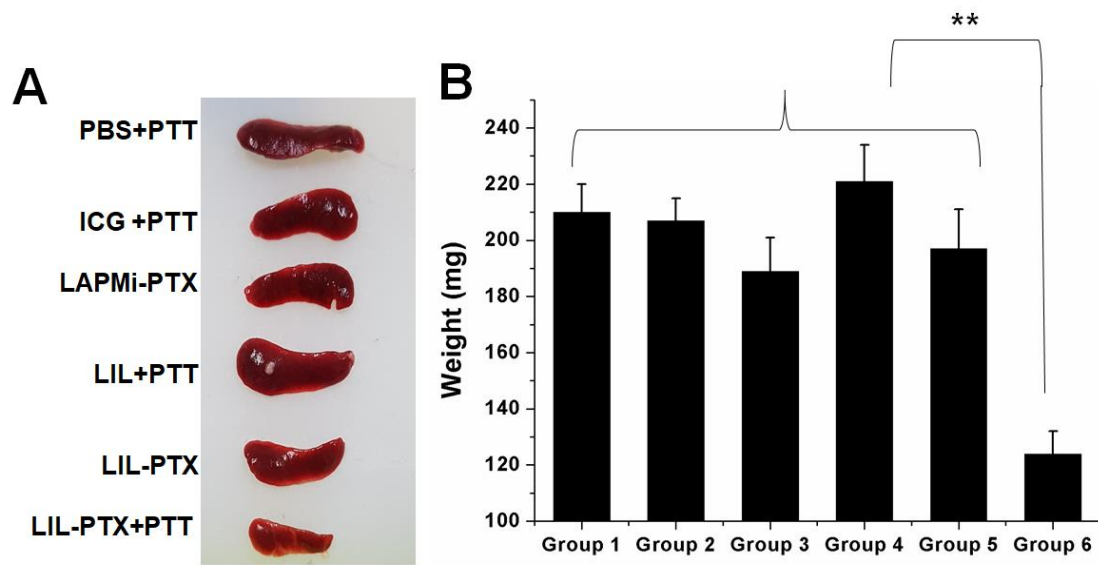


Figure S17. (A) Representative images of spleen collected from various groups after 14-day post-treatment. (B) Corresponding spleen weight. Group 1: PBS+PTT; Group 2: ICG+PTT; Group 3: LAPMi-PTX; Group 4: LIL+PTT; Group 5: LIL-PTX; Group 6: LIL-PTX+PTT (** $p < 0.01$).

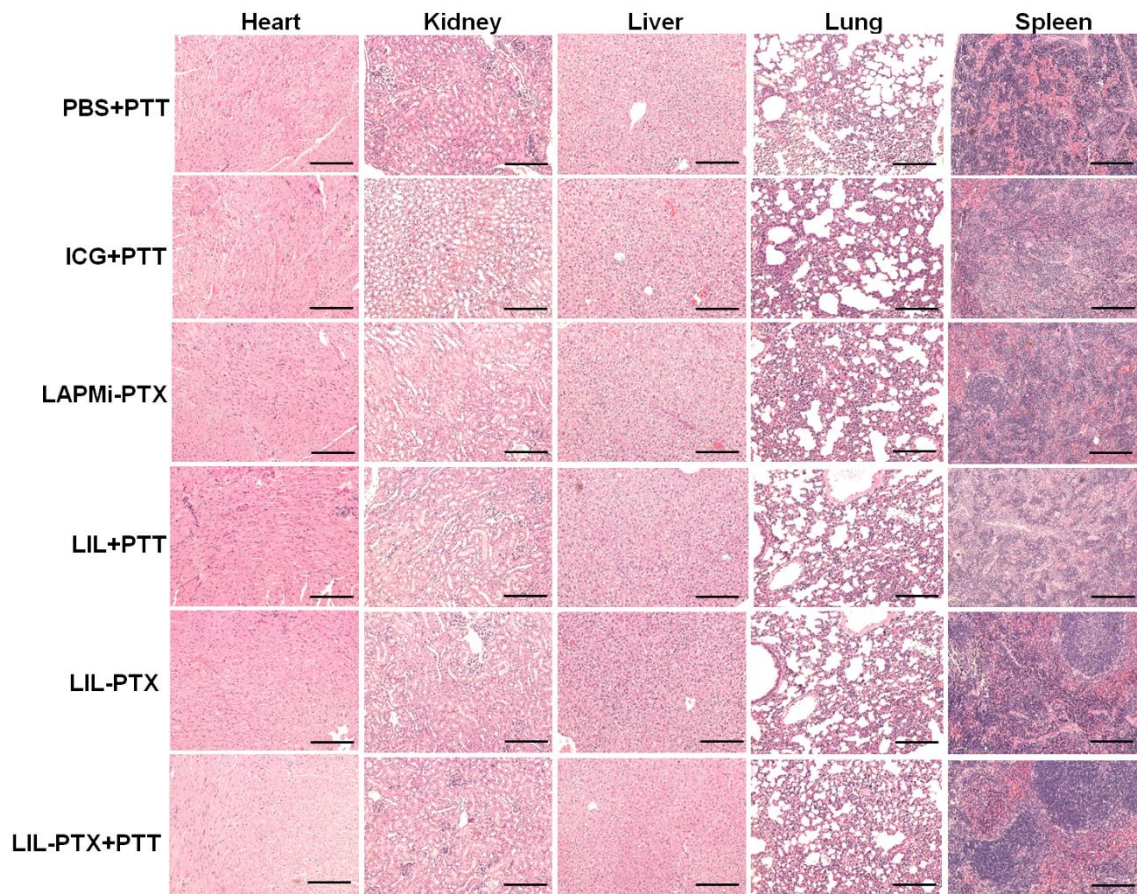


Figure S18. H&E stained organs collected from various groups on day 14 post-treatment.

Scale bar indicates 100 µm.

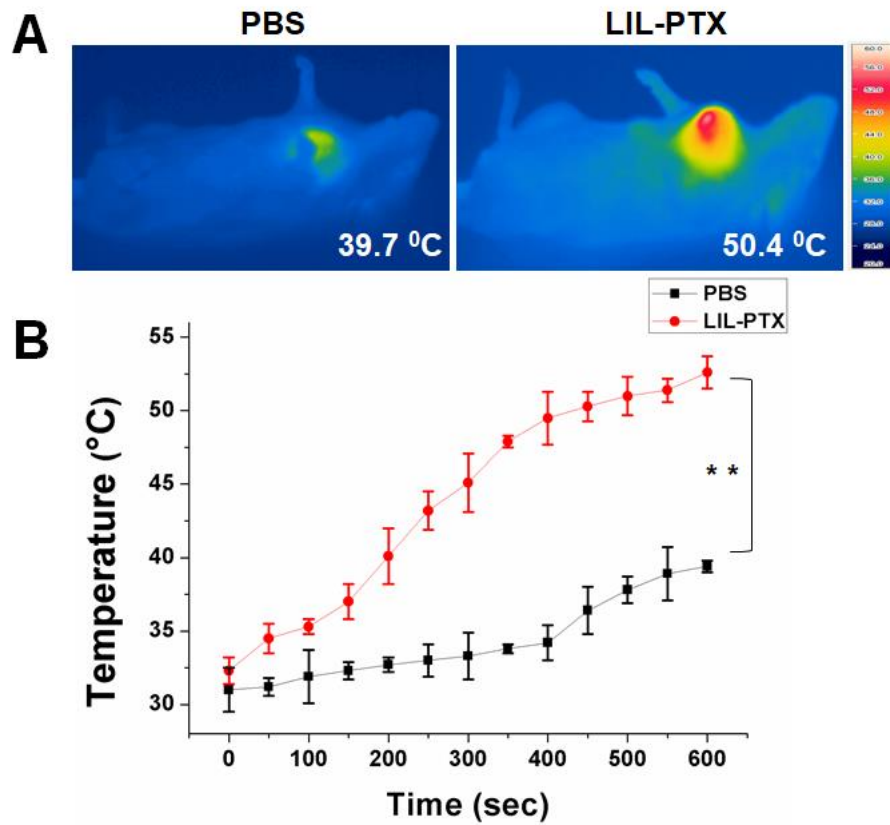


Figure S19. (A) Thermal images and (B) Thermal graph of 4T1 tumor bearing mouse with post-laser irradiation (808nm, 2W/cm², 10 min) after tail vein injection of PBS and LIL-PTX NPs (** $p < 0.01$).

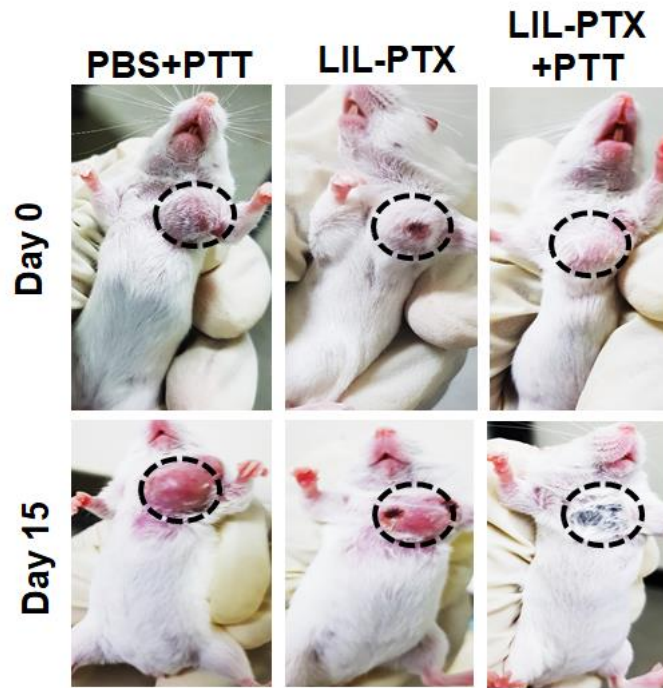


Figure S20. Representative images of 4T1 tumor bearing mice during treatment period.